- J. Phys. Chem. Lett. –
Spectroscopy and Photochemistry

Perpendicular State of an Electronically Excited Stilbene: Observation by Femtosecond Stimulated Raman Spectroscopy

Martin Quick[a], Alexander L. Dobryakov[a], Ilya N. Ioffe[b], Alex A. Granovsky[c], Sergey A. Kovalenko[a], Nikolaus P. Ernsting[a]**

[a] Department of Chemistry, Humboldt-Universität zu Berlin, Brook-Taylor-Str. 2, D-12489 Berlin, Germany

[b] Department of Chemistry, Lomonosov Moscow State University, Moscow, Russia

[c] Firefly Project, 117593 Moscow, Russia

*quickmaq@chemie.hu-berlin.de, nernst@chemie.hu-berlin.de

Supporting Information

Transient absorption (TA) measurements. Our setup with applications has been described elsewhere[1,2]. It provides spectral coverage 275 – 690 nm with 0.1 ps instrumental response (fwhm) over the full probe range and timing precision of 0.02 ps. A solution of 1,1'-dicyanostilbene in *n*-hexane (~ 0.1 mM) was flown through a sample cell of 0.4 mm internal thickness. Transient absorption spectra $\Delta A(\lambda, t)$ were recorded upon 351 nm excitation. 16 pump-probe scans were averaged to improve the signal-to-noise ratio. All TA spectra were recorded at the magic angle between pump- and probe polarizations.

Femtosecond-stimulated Raman (FSR) measurements. The transient Raman setup was similar to that for TA[3,4]. The narrow picosecond Raman-pump (0.1 μJ, 920 Hz) was tuned to $\lambda_R = 470$ nm or $\lambda_R = 510$ nm. The polychromator dispersion was adjusted to cover a 1000 cm^{-1} probe range. Stokes Raman signal was recorded by chopping the Raman-pump beam, with actinic excitation at $\lambda_{ac} = 340$ nm. In this registration scheme, signals at negative pump-probe delays correspond to ground-state Raman contributions from both solute and solvent. For positive delays these contributions are eliminated by subtracting the (averaged) signal from negative delays. 64 pump-probe scans were averaged to improve the signal-to-noise ratio. All FSR spectra were recorded at the 0° angle between pump- and probe polarizations.

The evolution of the transient absorption spectrum is discussed in the main text. In addition, the three kinetic traces shown in **Fig. S1** help to understand the evolution of *trans*-1,1'-dicyanostilbene in *n*-hexane upon excitation. *(a)*: ESA at 655 nm originates from S_1 after leaving the FC region and decays with $\tau_2 = 0.3$ ps. With the same time constant ESA from the P-state appears around 370 nm. — *(b)* The time trace at 500 nm represents both: the decay of ESA(R) with τ_2 and the decay of SE from an intermediate state X´ with $\tau_3 = 1$ ps. Additional rise with

τ_3 is noticed in *(a)* for ESA(P) and further population transfer from X′ to the P-state is concluded.

A comment is in order regarding the model fit, i.e. an oscillatory time function, 5 exponential time functions, and an offset. The criterion for using this set of time functions (and not 4 exponential functions, for example) was given by a rank analysis of the data matrix $\Delta A(\lambda,t)$. Altogether 7 linearly independent basis spectra, and hence, corresponding (but so far, unknown) time functions are needed to describe the measured data down to noise. Trial and error then led to the functional set above.

We note here that spectral shifts, in principle, need a more extended description. In our case the initial shift of the SE band in the course of vibrational relaxation is concerned (see **Fig. 1a**). A general description is available in the form of a Laplace transformation of kinetic traces for every probe wavelength. This is equivalent to using a distribution of time-exponentials with associated spectra. For given experimental data, however, the distribution may be replaced by a series of time-functions and associated spectra. This series can be recast into a succession of virtual states $A\rightarrow B\rightarrow C\rightarrow\ldots\rightarrow Z$. The associated spectra of the virtual states represent the essence of the spectral evolution. We find that "a series of two" terms is sufficient for the early spectral shift (160 fs) of the SE band in **Fig. 1**.

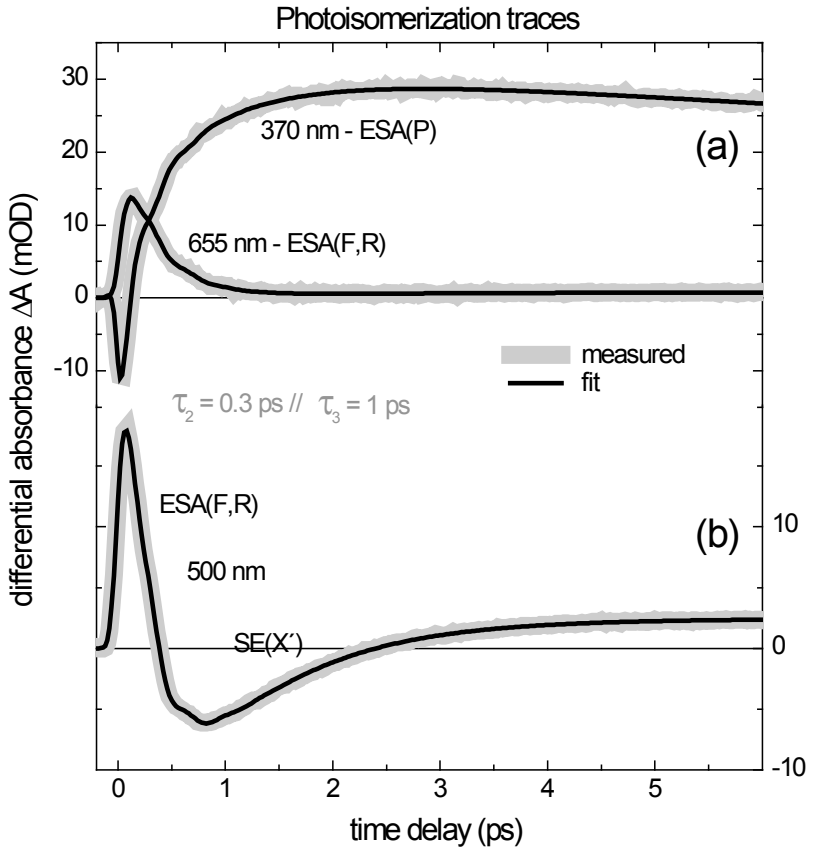

Figure S1.

(a) The trace at 655 nm describes the decay of ESA(F,R) $S_1 \rightarrow S_n$ with $\tau_2 = 0.3$ ps. The trace at 370 nm reflects the ESA(P) band. It rises with 0.3 and also with $\tau_3 = 1$ ps; it decays with $\tau_4 = 27$ ps (not shown).

(b) At 500 nm the decay of ESA(F,R) and the decay of red-shifted SE(X´) are seen to occur in sequence. In general, fits involve one oscillatory ($\nu = 100$ cm^{-1}) and four exponential time functions plus an offset.

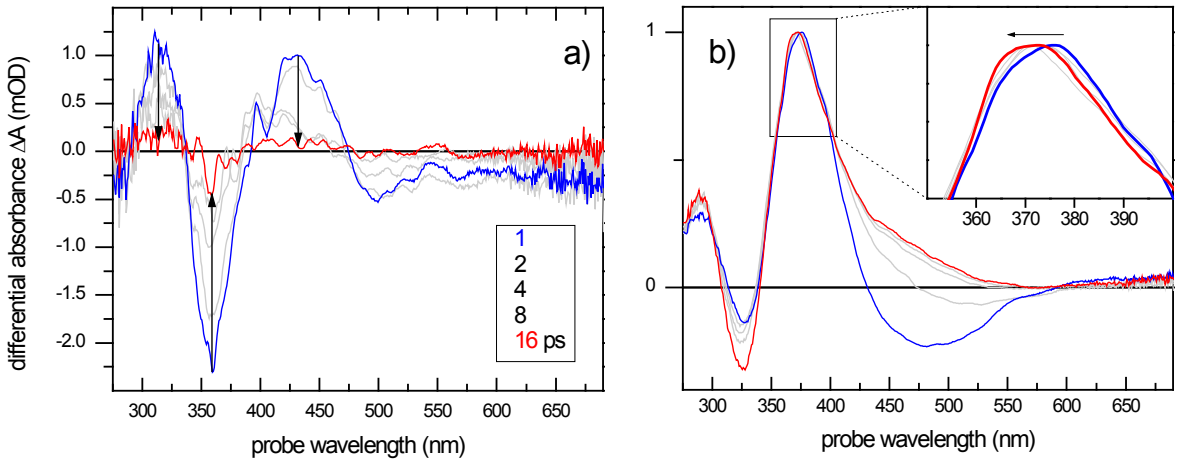

Figure S2.

Spectral change associated with the 7 ps relaxation process. *(a)* Shown is the residuum after subtraction of all other (properly weighted) time-functions. Bands in the regions 390 – 475 nm and 335 - 390 nm are responsible for a blue-shift of the P band by 280 cm^{-1}, probably due to cooling *(b)*. The feature at 310 nm is attributed to a component of ground-state recovery.

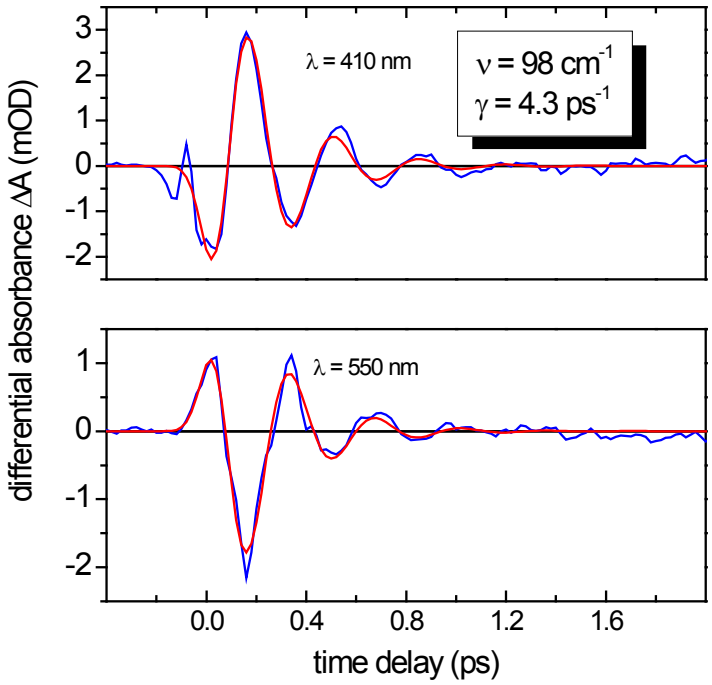

Figure S3.

Oscillation in transient absorption traces after all other fit data have been subtracted. Measured oscillatory traces (blue) and fits (red) are shown for $\lambda = 410$ and 550 nm. The oscillation wavenumber is $\nu = 98$ cm^{-1} and the decay rate $\gamma = 4.3$ ps^{-1}. We speculate that phenyl torsional motion is seen here.

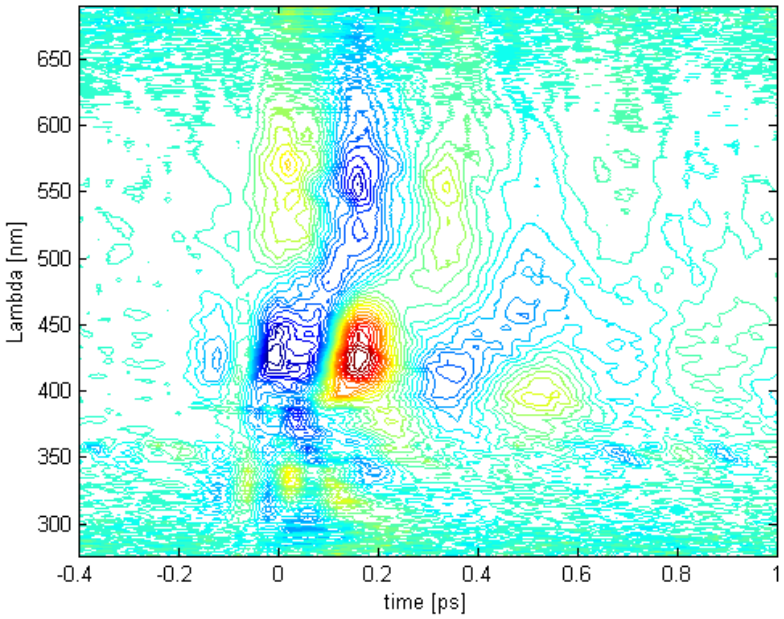

Figure S4.

The wavelength-dependent oscillation behavior in the TA data exhibits a phase shift by π around 490 nm. The underlying electronic absorption band, which is being frequency modulated here, must therefore have its peak at 490 nm. Most likely a corresponding ESA band (local maximum) in **Fig. 1b** is involved.

The non-resonant FSR spectrum of 1,1'-dicyanostilbene in the electronic ground state is shown in **Fig. S4**. It was recorded with λ_R = 510 nm. Parts of the spectrum are magnified with a factor 10. Vertical bars indicate the positions of measured S_0 Raman signals of *trans*-stilbene for comparison [4]. The two most intense Raman lines at 1549 and 1590 cm^{-1} are attributed to ethylenic C=C-stretching modes, as follows from a correspondence with lines from *trans*-stilbene and 1596 and 1639cm^{-1}.

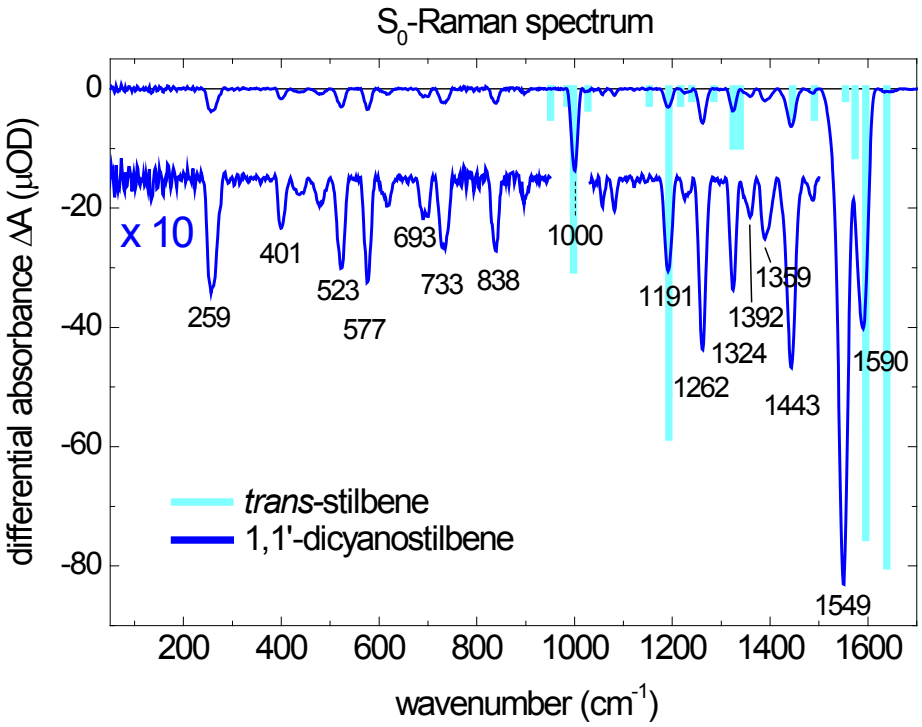

Figure S4. S_0-Raman spectrum of 1,1'-dicyanostilbene in *n*-hexane was recorded with 510 nm Raman excitation on the Stokes-side. The strongest Raman activity is observed in the high-frequency region at 1549 and 1590 cm^{-1}. The comparison with measured S_0-Raman lines of *trans*-stilbene in *n*-hexane allows their identification as C=C-stretching modes of the ethylenic center and phenyl groups [4].

Raman lines of the P-state are identified via their life time, τ_4 = 27 ps. The decay is seen in **Fig. 5d** of the main text where selected signals are shown for delay times 10, 20 and 30 ps. However, even with 64 recorded pump-probe scans the signal-to-noise ratio is poor for Raman signals from the P-state. This can be seen by the time trace, in **Fig. S5**, for the Raman signal at 1558 cm^{-1}. The

rise of the signal is not directly observable in FSR measurements with $\lambda_R = 510$ nm and $\lambda_R = 470$ nm because it is superimposed by decaying Raman signals in the relaxed S_1-state.

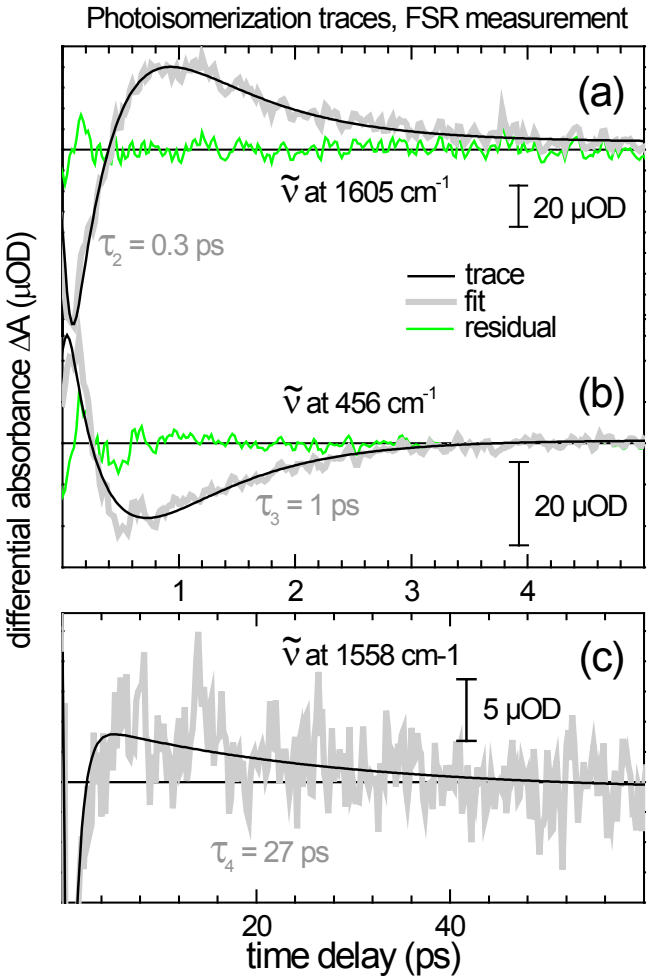

Figure S5. The traces shown originate from measurements with $\lambda_R = 470$ nm. — *(a)* The trace at 1605 cm^{-1} interrogates the negative part of a Raman line that decays fast with $\tau_2 = 0.3$ ps. — *(b)* As representative for negative signals in state X´ the kinetic trace at 456 cm^{-1} is shown. Optical density is positive first, then turns negative at 0.2 ps forming

the line under discussion, and finally decays with $\tau_3 = 1$ ps. — *(c)* The decay of Raman signal from the perpendicular state P is demonstrated here shown for the positive part of the line at 1558 cm^{-1}. The decay proceeds with $\tau_4 = 27$ ps. With an optical density of only a few μOD the Raman-signal amplitude, when taken by itself, ranges close to the noise level. Since the electronic background behaves with the same time-constants, kinetic traces of this quality can be easily be caused by background intensity that was not removed accurately. But when the spectral signature is monitored in addition, the S/N ratio is much improved. For this reason the evolution of weak Raman lines was presented in **Fig. 5d** in form of spectra at different delay times.

Photoproduct(s) are formed by a small fraction of the initially excited population. They can be seen as an offset in the TA- and FSR-spectrum which remains at the longest delay time. In **Fig. 5d** this offset has been subtracted in order to focus on the decay of signal from the P-state. No such subtraction has been performed for **Fig. S6** below. Furthermore, here the electronic background has been removed in such a way that vibrational activity is entirely treated as negative lines (as is indeed the case for S_0 signals of photo-products). The formation of the photo-product is recognized most easily through lines at 348 and 1574 cm^{-1}. — *Top panels*: The time range 0.1 – 0.4 ps represents the window in which evolution takes place with $\tau_2 = 0.3$ ps. No rise of lines from the photo-product is observed here. — *Middle panels*: Evolution with $\tau_3 = 1$ ps is represented in the time window 0.4 – 1.6 ps. Here lines from a photoproduct emerge, which is best seen for 1574 cm^{-1}. — *Bottom panels*: These lines remain constant within the first 20 ps and are therefore distinguishable from decaying signals in the P-state.

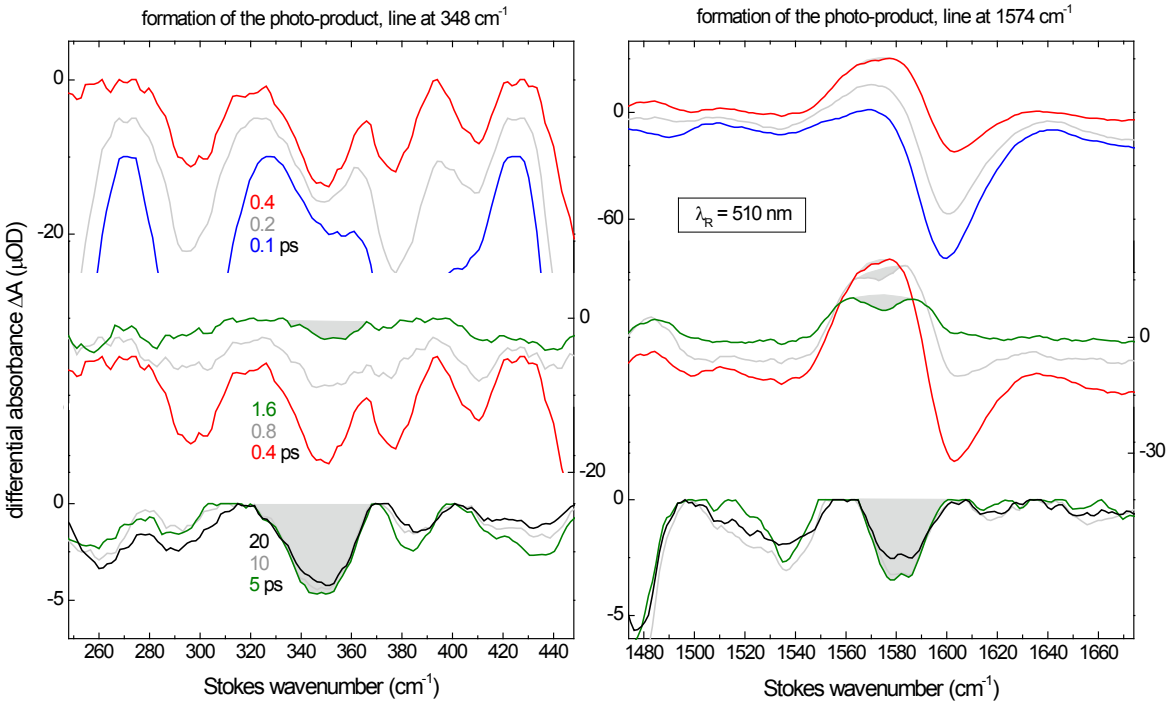

Figure S6. The rise of S_0-Raman signals from a photoproduct is shown for example at 348 and 1574 cm^{-1}. *Top*: No signals emerge on the fast time-scale (0.1 – 0.4 ps). Middle: Negative lines show up on the time scale 0.4 – 1.6 ps as signals from X´ vanish. *Bottom*: Their intensities remain constant while signals in the P-state decay.

On the signal-to-noise ratio in FSR spectra. To observe Raman signals of the P-state we first used picosecond pulses at λ_R = 388 nm that are directly available in our setup[3]. For optical probing in the Stokes range 388 – 417 nm (~ 1800 cm^{-1}) a super-continuum was generated by self-phase modulation (SPM) in a CaF_2 crystal. A major disadvantage of this arrangement is a lack of suitable photon flux for probing. To efficiently generate probe pulses for FSR spectroscopy in our laboratory, we currently need NOPA technology. In this case our spectral range is restricted to 470 - 700 nm, which implies pre-resonant conditions in regard to the

perpendicular state P. In the main text we reported Raman lines of P which were measured in this way. The question remains, why are results recorded (i) under pre-resonance conditions with NOPA probing, better than those recorded (ii) resonantly upon 388 nm Raman excitation with super-continuum probing?

In **Fig. S7** both experimental arrangements (i, ii) are used in an attempt to record excited-state FSR spectra of 1,1'-dicyanostilbene in *n*-hexane. The delay time $t_d = 5$ ps is chosen when the P-state is populated and photoproduct(s) have been formed. S_0 contributions (of 1,1'-dicyanostilbene and *n*-hexane) have been subtracted. Each spectrum is recorded twice and results are plotted below one another. *Top*: With $\lambda_R = 388$ nm and supercontinuum probing, successive spectra show fluctuations on the order of several 100 μOD. The fluctuations do not indicate vibrational activity because of their large width (~ 100 cm^{-1}) and lack of reproducibility. The noise is increasing towards longer wavelengths from 20 to 150 μOD. *Bottom*: With $\lambda_R = 470$ nm and probes from NOPA sources, each pair of spectra shows good correlation so that recurring narrow structure can be identified as a vibrational band. The noise level remains constant at about 4 μOD throughout.

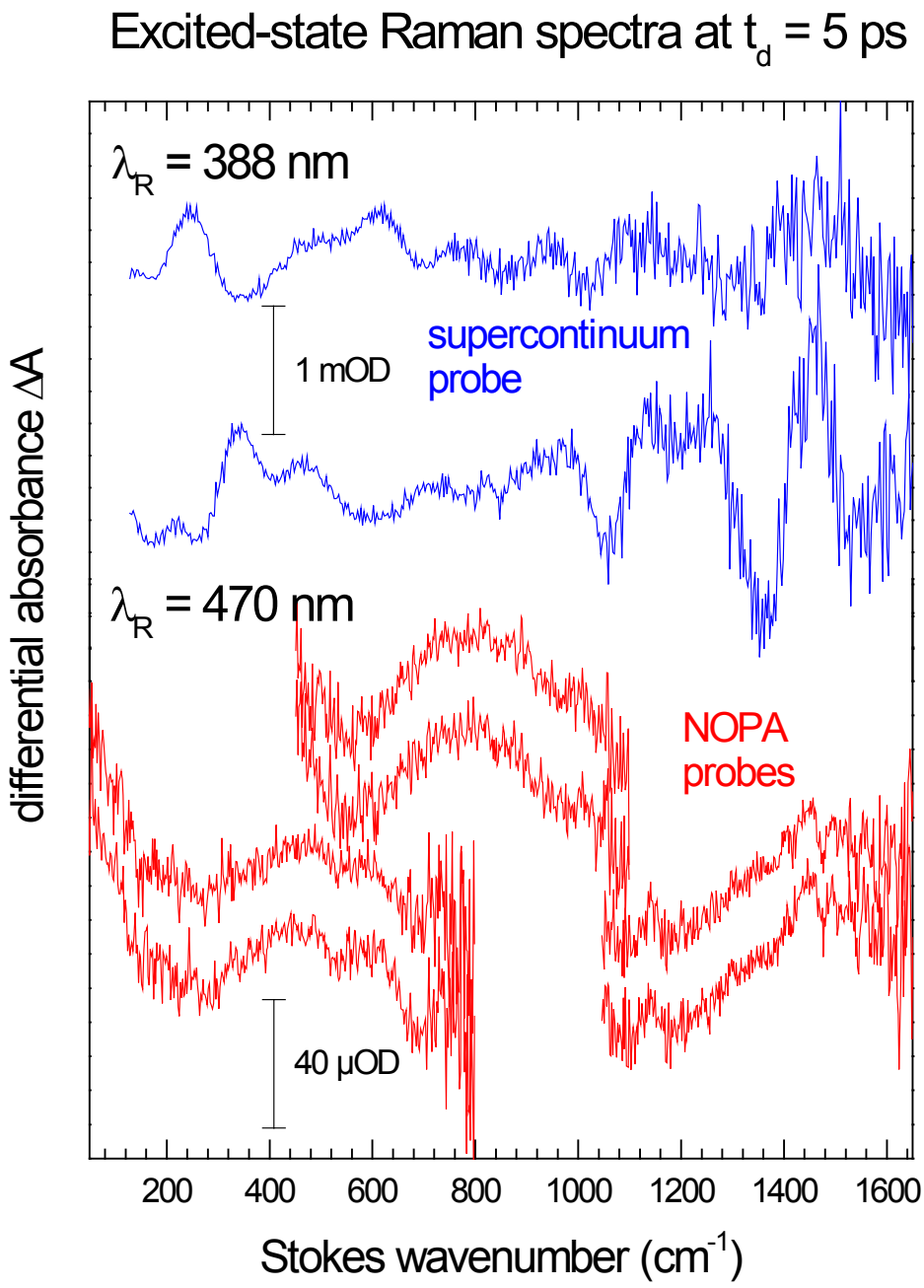

Figure S7. Attempts to record excited-state Raman spectra with different Raman pump/probe combinations. 1,1'-dicyanostilbene in n-hexane at t = 5 ps was used; *cf.* text.

Intensity profiles of the probe-pulses that enter the reference spectrograph are shown in **Fig. S8**. The profiles are the result of an average of 200 individually recorded spectra. The standard-deviation at each spectral position is added and subtracted (light lines) to the profile, forming a band for visualization of relative noise. In the following we compare white-light, supercontinuum probe pulses (blue) with short Fourier-transform limited pulses (red) from a NOPA source.

Two properties determine the quality of Raman spectra which are recorded with such probe pulses. The first is the intensity variation across the probe pulse. For example the super-continuum is bright around the generating wavelength (388 nm) but small at longer wavelengths. For comparison consider a sum of well-placed NOPA pulses. The resulting synthetic aperture for probing can be tailored to cover the Stokes window evenly. As a consequence, the dynamic range of detection can be used fully across the Stokes window, so that relative noise for Raman signal is low. The second property are the relative fluctuations by themselves. The variance of probe intensity enters *as a factor* into the confidence interval $CI_{\Delta A}$ for induced absorbance changes, as was shown in ref. (2) (the other factor $\sqrt{1-\gamma}$ is determined by the sample-reference intensity correlation γ). As a consequence, $CI_{\Delta A}$ is about 20-100 times smaller with NOPA probing compared to super-continuum probing. $CI_{\Delta A}$ sets the noise floor for the detection of Raman-induced lines. To conclude, the noise-equivalent power of Raman lines must be about 20-100 times larger with (our) supercontinuum probing, compared to NOPA probing.

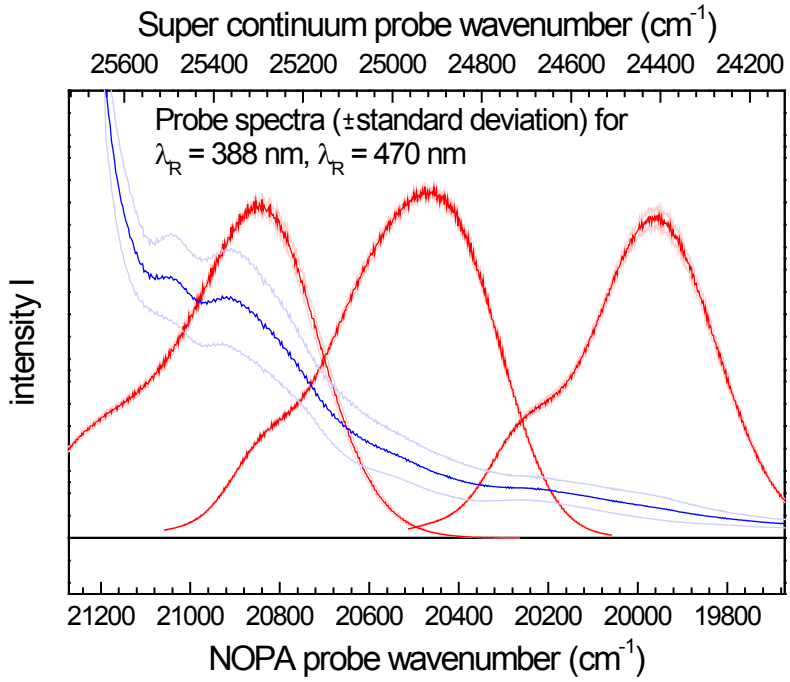

Figure S8. Shown are the intensity profiles of the generated probe-beams as recorded in the reference spectrograph. For $\lambda_R = 388$ nm the probe-light is generated by focusing the 388 nm-beam on a moving CaF_2-plate (centered at 388 nm, blue). For $\lambda_R = 470$ nm it is generated in a NOPA process (centered at 394, 400 and 409 nm, red). All profiles are an average of 200 recorded spectra and the standard deviation at each point is added and subtracted from the profiles, respectively, which yield two light lines (one up and one below).

Not only has the confidence interval CIΔA suffered from the broad-band continuum as source for the probe-light. Also the expected gain of Raman-intensity could be over-compensated by inappropriate experimental conditions. In **Fig. S9** the S_0 spectrum of a mixture

of toluene and acetonitrile (volume ratio 1:1) is shown with $\lambda_R = 388$ nm and $\lambda_R = 470$ nm, respectively, each having a pump-energy of 100 nJ per pulse. With 470 nm Raman excitation the Raman line at 1003.6 nm of toluene appears with an optical density of 8 mOD on the Stokes-side. With the $S_0 \rightarrow S_1$ transition at ~267 nm a larger Raman signal is expected with 388 nm Raman excitation since it comes closer to this resonance. However, less than 4 mOD were recorded in the best case. The signal intensity strongly depends on the focusing of the 388 nm fs-pulse that generates the super-continuum in the CaF_2 plate.

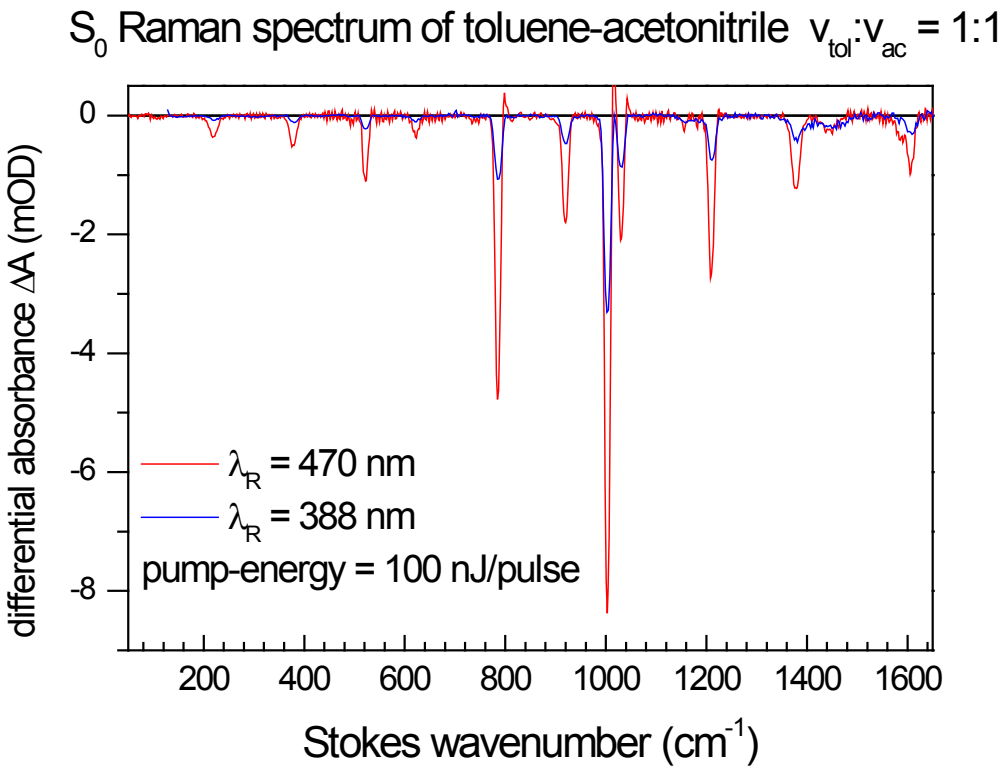

Figure S9. S_0 Raman spectra of a mixture of toluene and acetonitrile ($vol_{tol}/vol_{ac} = 1:1$) recorded with $\lambda_R = 388$ nm and $\lambda_R = 470$ nm excitation. Even though the power of the Raman pump was equal in the experiments, more intense signals are observed for the longer excitation wavelength.

References

(1) Kovalenko, S. A. ; Dobryakov, A. L.; Ruthmann, J.; Ernsting, N. P. Femtosecond Spectroscopy of Condensed Phases with Chirped Supercontinuum Probing. *Phys. Rev. A*, **1999**, *59*, 2369-2384.

(2) Dobryakov, A. L.; Kovalenko, S. A.; Weigel, A.; Perez-Lustres, J. L.; Lange, J.; Müller, A.; Ernsting, N.P. Femtosecond Pump/Supercontinuum-Probe Spectroscopy: Optimized Setup and Signal Analysis for Single-Shot Spectral Referencing. *Rev. Sci. Instrum.* **2010**, *81*, 113106.

(3) Kovalenko, S. A.; Dobrykov, A. L.; Ernsting, N. P. An Efficient Setup for Femtosecond Stimulated Raman Spectroscopy. *Rev. Sci. Instum.* **2011**, *82*, 063102, 1-10.

(4) Dobryakov, A. L.; Ioffe, I.; Granovsky, A. A.; Ernsting, N. P.; Kovalenko, S. A. Femtosecond Raman Spectra of cis-stilbene and trans-stilbene with Isotopomers in Solution. *J. Chem. Phys.* **2012**, *137*, 244505, 1-16.